Reactions of interstitial carbon with impurities in silicon particle detectors

L. F. Makarenko[a)]
Department of Applied Mathematics, Belarusian State University, 220030 Minsk, Belarus

M. Moll
CERN PH-DT2-SD, CH-1211 Geneva 23, Switzerland

F. P. Korshunov and S. B. Lastovski
Institute of Solid State and Semiconductor Physics, 220072 Minsk, Belarus

(Received 29 November 2006; accepted 24 April 2007; published online 14 June 2007)

We present deep level transient spectroscopy (DLTS) data measured on very high resistivity *n*-type float-zone silicon detectors after irradiation with 6 MeV electrons. The carbon interstitial annealing kinetics is investigated as a function of depth in the detector structure and related to the inhomogeneous depth distribution of oxygen and carbon impurities in the devices. We compare our results with data published in previous works and point out some possible misinterpretation of DLTS data due to detector processing induced inhomogeneous distribution of impurities. Finally, we present a method to determine the absolute concentration of the oxygen and carbon impurities as functions of depth in devices by carefully analyzing the carbon interstitital annealing kinetics.
 [DOI: 10.1063/1.2745328]

I. INTRODUCTION

Modeling of radiation induced defect kinetics plays an important role in finding ways to improve radiation hardness of silicon particle detectors. It helps, first, to test our current understanding of damage processes in detector structures and, second, to predict effects of different impurities on radiation damage. Modeling is therefore an indispensable tool for a successful defect engineering approach.

Several works have been performed on the simulation of radiation induced defect formation and their influence on silicon detectors characteristics.[1–6] They are all based on the model of impurity-defect interactions suggested in Ref. 7 An essential part of this model are interstitial carbon (C_i) reactions. These are responsible for the formation of interstitial-type defect complexes which are stable at room temperature (RT).

The simulation of C_i reactions is based on three assumptions.

(1) Substitutional carbon (C_s) atoms are the main traps for silicon interstitials in high resistivity silicon crystals.
(2) Only isolated carbon atoms in interstitial position are the source of mobile carbon species responsible for the formation of carbon related complexes stable at room temperature.
(3) The kinetics of their formation at low irradiation fluences is controlled by the C_i diffusion coefficient and C_i capture radii by oxygen, substitutional carbon, and doping impurities (phosphorus, etc.).

The first assumption is valid when the concentration of boron is about two orders of magnitude less than the carbon concentration. This was confirmed by many studies of Si crystals having a relatively low doping concentration, i.e., rather high resistivities.[8]

However, the last two assumptions have so far not received an unambiguous experimental confirmation. The second assumption has been called in question for detector grade Si.[9] The third assumption concerns the activation energy of C_i annealing (E_{ann}) and the influence of carbon and oxygen content on the annealing rate. As pointed out in Ref. 10, there is an unexplained scattering of experimental data for E_{ann} obtained by different authors. Similarly, a wide range of capture radii ratios has been reported for different impurities.[7,11–13]

Therefore, more experimental work on the basic aspects of interstitial carbon reactions is needed to further improve the defect kinetics modeling. In this paper, we try to elucidate some of the discrepancies reported in the literature and we contribute experimental data to further support the second and third assumptions given above.

II. EXPERIMENTAL DETAILS

In this work detector structures made by ST Microelectronics, Catania, Italy from high resistivity ⟨100⟩ and ⟨111⟩ *n*-type 6 in. float-zone (FZ) silicon wafers produced by Wacker Siltronic, Burghausen, Germany were used. The material resistivity determined from capacitance-voltage measurements was 2 kΩ cm. Simple p^+-*n*-n^+ structures with one guard ring were used. The basic process steps of their fabrications were typical to silicon planar technology: thermal oxidation, photolithography, ion implantation with subsequent annealing for impurity activation, and metallization. A more detailed description of the detector structures and their fabrication is presented in Ref. 14

Irradiation with electrons with an energy of 6 MeV was done using an accelerator at the Institute of Solid State and

[a)]Electronic mail: makarenko@bsu.by

Semiconductor Physics, Minsk, Belarus. The irradiation fluence was $\Phi = 1 \times 10^{12}\ e/\mathrm{cm}^2$. The irradiated samples were subjected to isothermal annealing in the temperature range of 40–70 °C.

Annealing processes have been studied using capacitance deep level transient spectroscopy (DLTS) ($T_{\mathrm{meas}} = 77$–325 K). The experimental equipment consisted of a capacitance meter, a 1 MHz HF generator, a dc source, a pulse generator, and personal computers, which controlled the pulse generator and performed the data acquisition. If not mentioned otherwise, a rate window setting of 190 s^{-1} was used.

Capacitance-voltage measurements were carried out with a capacitance bridge at room temperature. The capacitance has been measured at different reverse bias values by superimposing an ac voltage on the dc voltage, assuming a parallel mode equivalent circuit. The reverse bias is typically varied in the range $V_R = 0$–150 V in steps of 0.045–0.135 V. The amplitude and frequency of the ac voltage were 25 mV and 1 MHz, respectively. The measurements were controlled by a computer program and a custom made instrument interface.

III. DESCRIPTION OF ANNEALING KINETICS FOR INTERSTITIAL CARBON

Taking into account the three basic assumptions about the carbon interstitial reactions given in the Introduction, the following two concurrent reactions of interstitial carbon are dominant in high resistivity silicon:

$$\mathrm{C}_i + \mathrm{O}_i \rightarrow \mathrm{C}_i\mathrm{O}_i, \tag{1}$$

$$\mathrm{C}_i + \mathrm{C}_s \rightarrow \mathrm{C}_i\mathrm{C}_s. \tag{2}$$

According to Ref. 8, these reactions will be dominant for low radiation levels when the concentration of radiation induced defects is significantly lower than the concentration of carbon. For detector grade silicon, carbon and oxygen concentrations are typically about 5×10^{15} cm^{-3} (see, for example, Ref. 2). The DLTS method is usually applied when defect concentrations are at least about 10% or less than those of doping impurities. Therefore, the conditions for the domination of reactions (1) and (2) are always fulfilled for the diodes under study.

The rate of these reactions can be described by the following equations:

$$\frac{d[\mathrm{C}_i\mathrm{O}_i]}{dt} = K_{\mathrm{CO}}[\mathrm{C}_i] \cdot [\mathrm{O}_i], \tag{3}$$

$$\frac{d[\mathrm{C}_i\mathrm{C}_s]}{dt} = K_{\mathrm{CC}}[\mathrm{C}_i][\mathrm{C}_s], \tag{4}$$

where K_{CO} and K_{CC} are the interaction coefficients of C_i with O_i and C_s, respectively.

Assuming that only the $\mathrm{C}_i\mathrm{C}_s$ and the $\mathrm{C}_i\mathrm{O}_i$ defects can be formed from C_i, the elimination rate of C_i and the growth rate of the other complexes are connected by

$$\frac{d[\mathrm{C}_i]}{dt} = -\frac{d[\mathrm{C}_i\mathrm{C}_s]}{dt} - \frac{d[\mathrm{C}_i\mathrm{O}_i]}{dt}. \tag{5}$$

Assuming that $[\mathrm{C}_i] \ll [\mathrm{C}_s]$, $[\mathrm{O}_i]$ one obtains

$$[\mathrm{C}_i] = [\mathrm{C}_i]_{\max} \exp\left(-\frac{t}{\tau_{\mathrm{ann}}}\right), \tag{6}$$

$$[\mathrm{C}_i\mathrm{C}_s] = [\mathrm{C}_i\mathrm{C}_s]_{\max}\left\{1 - \exp\left(-\frac{t}{\tau_{\mathrm{ann}}}\right)\right\}. \tag{7}$$

Here, $\tau_{\mathrm{ann}}^{-1} = K_{\mathrm{CC}}[\mathrm{C}_s] + K_{\mathrm{CO}}[\mathrm{O}_i] \equiv \tau_{\mathrm{CC}}^{-1} + \tau_{\mathrm{CO}}^{-1}$ is the effective interstitial carbon annealing rate and $[\mathrm{C}_i]_{\max}$ and $[\mathrm{C}_i\mathrm{C}_s]_{\max}$ are the initial and final concentrations of C_i and $\mathrm{C}_i\mathrm{C}_s$, respectively.

The following equations can be easily obtained from Eq. (3)–(7):

$$[\mathrm{C}_i\mathrm{C}_s] = [\mathrm{C}_i\mathrm{C}_s]_{\max} - \frac{[\mathrm{C}_i\mathrm{C}_s]_{\max}}{[\mathrm{C}_i]_{\max}}[\mathrm{C}_i] \tag{8}$$

and

$$\frac{\dfrac{d[\mathrm{C}_i\mathrm{C}_s]}{dt}}{\dfrac{d[\mathrm{C}_i]}{dt}} = \frac{K_{\mathrm{CC}}[\mathrm{C}_s]}{K_{\mathrm{CC}}[\mathrm{C}_s] + K_{\mathrm{CO}}[\mathrm{O}_i]} = \frac{\tau_{\mathrm{CC}}^{-1}}{\tau_{\mathrm{ann}}^{-1}} = \frac{[\mathrm{C}_i\mathrm{C}_s]_{\max}}{[\mathrm{C}_i]_{\max}} \equiv \eta. \tag{9}$$

The knowledge of η and τ_{ann} allows us therefore to evaluate both partial annealing rates τ_{CC}^{-1} and τ_{CO}^{-1} as

$$\tau_{\mathrm{CC}}^{-1} = K_{\mathrm{CC}}[\mathrm{C}_s] = \eta\tau_{\mathrm{ann}}^{-1} \tag{10}$$

and

$$\tau_{\mathrm{CO}}^{-1} = K_{\mathrm{CO}}[\mathrm{O}_i] = (1 - \eta)\tau_{\mathrm{ann}}^{-1}. \tag{11}$$

Using Eqs. (6) and (8) on a complete set of C_i annealing data yields the two parameters: τ_{ann}^{-1} and η and accordingly the values $(K_{\mathrm{CO}}[\mathrm{O}_i])$ and $(K_{\mathrm{CC}}[\mathrm{C}_s])$.

IV. EXPERIMENTAL RESULTS AND THEIR INTERPRETATION

A standard procedure to extract an annealing time is an isothermal annealing experiment. In our experiment we performed isothermal annealing studies at two temperatures for each sample. Typical DLTS spectra obtained for such kind of experiment are shown in Fig. 1. Two of the presented traps, E0 and H1, have previously been identified as the acceptor and donor states of C_i, respectively.[10]

The annealing behavior of the DLTS spectra was the same irrespective of which temperature (the lower or the higher) had been applied first and irrespective of crystal orientation. In any case, the amplitudes of the E0 and H1 peaks decrease while the amplitudes of E1 and H2 peaks increase. The DLTS peak E1 is due to the superposition of the signals arising from vacancy-oxygen (VO) and substitutional carbon interstitial carbon complexes ($\mathrm{C}_i\mathrm{C}_s$).[10,14] The hole trap signal H2 is related to interstitial oxygen interstitial carbon complexes ($\mathrm{O}_i\mathrm{C}_i$).[14]

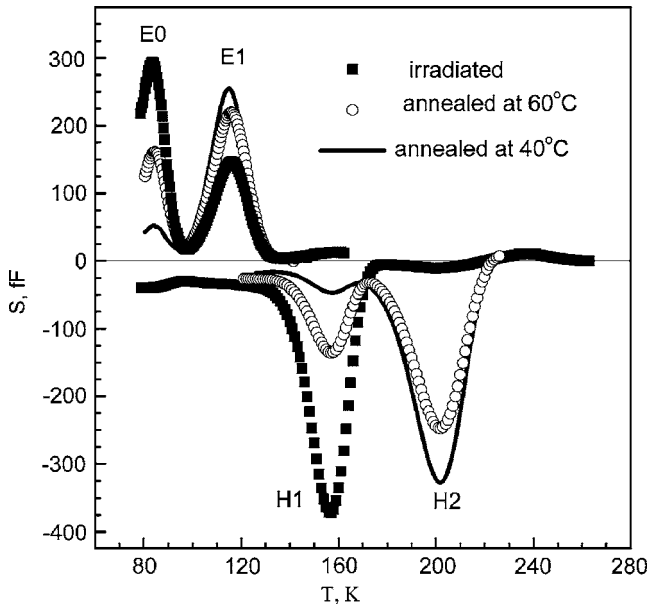

FIG. 1. DLTS spectra obtained immediately after irradiation with 6 MeV electrons and subsequent annealing, first, at 60 °C and, second, at 40 °C. The crystal orientation is ⟨100⟩.

Employing the three assumptions given in the Introduction, a simple exponential decay of the E0 peak amplitude is expected. As seen in Fig. 2, there is also a dependence of the decay rate on the bias used for measuring the DLTS spectra. Although the E0 and the H1 peaks originate from the same defect, a higher decay rate for the H1 peak is observed in the two investigated types of test structures.

Varying the reverse voltage and the filling pulse amplitude of DLTS measurements, we can investigate different depth regions of a diode structure. The higher the reverse voltage, the deeper is the region of the diode that is traced. As can be seen in Fig. 2, the closer the monitored region is to the surface, the higher is the normalized annealing rate of C_i. This is also expressed in Fig. 3 which shows the unannealed fraction of the C_i (E0) trap as a function of depth after 400 min annealing at 60 °C for two samples with different crystal orientations.

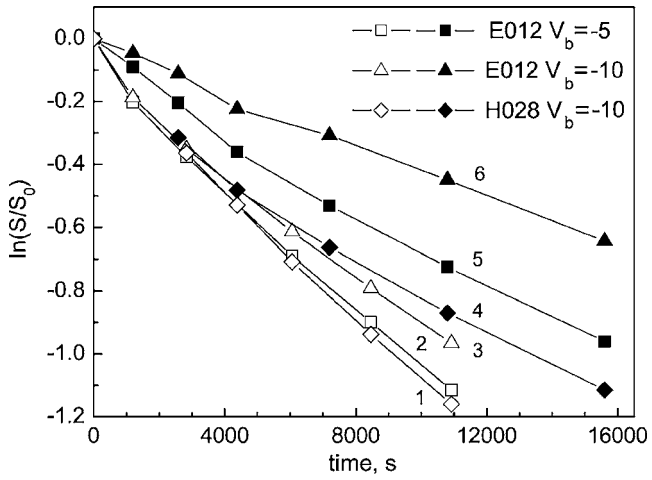

FIG. 2. Annealing kinetics of H1 (1,4) and E0 (2,3,5,6,) peaks in FZ detector. DLTS signal was measured at different bias voltages −5 V (2,5) and −10 V (1,3,4,6) for ⟨111⟩ (filled symbols) and ⟨100⟩ (empty symbols). The filling pulse amplitude was 5 V. The annealing temperature was 60 °C.

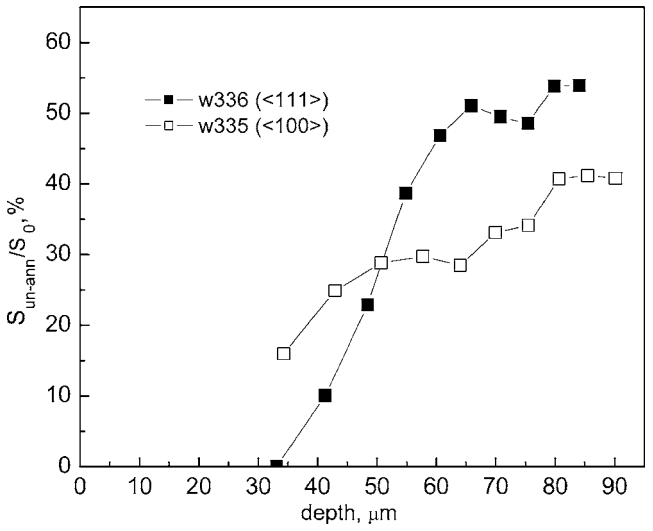

FIG. 3. Depth dependence of unannealed fraction of E0 trap in ⟨111⟩ (filled symbols) and ⟨100⟩ (empty symbols) detectors after annealing at 60 °C for 400 min.

For the diode with ⟨111⟩ crystal orientation the unannealed fraction of the E0 trap increases strongly with depth from about 35 to 65 μm. This may be first of all explained by the oxygen depth profile arising from the oxygen penetration into the structures during their processing. Presumably, oxygen diffuses into detectors during thermal oxidation, which takes place at temperatures of about 1000 °C or higher. Inhomogeneous oxygen distribution in standard silicon detectors was found earlier using secondary ion mass spectrometry (SIMS) measurements.[15]

The depth dependence of the C_i annealing rate in ⟨100⟩ diodes is less pronounced. This is evidence that there is a difference for oxygen penetration into ⟨100⟩ and ⟨111⟩ substrates which may be related to different conditions at the $Si-SiO_2$ boundary rather than anisotropic oxygen diffusivity (see Ref. 16 and references therein).

As is evident from the above presented data, an inhomogeneous distribution of C_i annealing rates may lead to errors in the determination of τ_{ann}^{-1} if the standard DLTS measurement procedure is used. In order to obtain a reliable value for the activation energy of C_i annealing (E_{ann}), it is therefore best to use DLTS spectra obtained for diode regions with as low as possible impurity gradients.

Figure 4 shows the kinetics of the C_i decay measured by subsequent annealing of the same samples at two different temperatures. The activation energy in this case may be determined similar to the "slopes method" described in Ref. 17 This method involves the sudden alteration of the annealing temperature during the annealing of the same sample and may be used even for nonexponential defect annealing.[16] The activation energy can be determined from the relation

$$E_{\text{ann}} = \frac{k_B \ln(R(T_2)/R(T_1))}{1/T_1 - 1/T_2}, \tag{12}$$

where $R(T_1)$ and $R(T_2)$ are the slopes of $[C_i]$ vs t curves constructed on both sides of kink points (Fig. 4). In practice, it is somewhat difficult to construct an accurate slope. Therefore, it is preferable to choose experimental conditions when

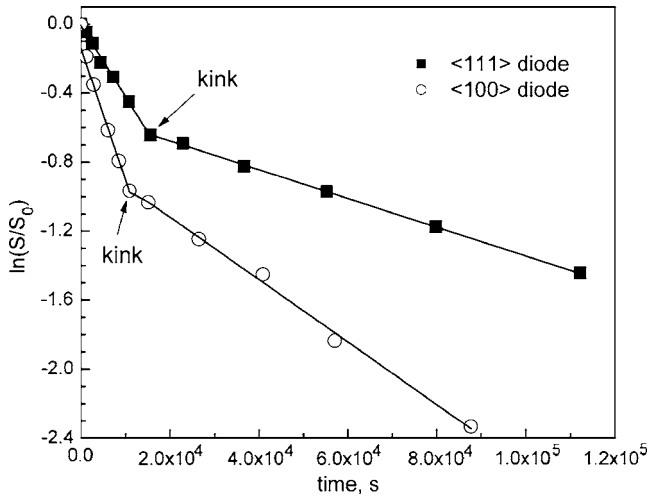

FIG. 4. Decay of E0 peak vs time of annealing at 60 °C (before the kink) and 40 °C (after the kink). The DLTS signal was measured at a bias voltage of −10 V for ⟨111⟩ (filled symbols) and ⟨100⟩ (empty symbols) detectors. The filling pulse amplitude was 5 V.

defect annealing obeys the exponential law. If that is the case, a relation $R(T_2)/R(T_1)=\tau_{\mathrm{ann}}^{-1}(T_2)/\tau_{\mathrm{ann}}^{-1}(T_1)$ is fully valid with inverse annealing times determined from straight lines representing $\ln([C_i])$ vs t dependencies. This allows us to determine E_{ann} more accurately. Using this procedure for several samples, we obtained the value of $E_{\mathrm{ann}} \approx (0.72\pm0.05)$ eV, which is consistent with the majority of results reported earlier.[9–11]

To determine the value of η we can use the data presented in Fig. 5, where a good correlation between the concentrations of E0 and E1 is observed if the very first points directly after irradiation ("as irradiated") are not taken into account. The sudden increase of the E1 trap concentration after the first annealing step is assumed to be caused by the formation of VO complexes from close metastable vacancy and oxygen pairs as described in Refs. 18 and 19 and references therein. This process is thus not related to the carbon kinetics.

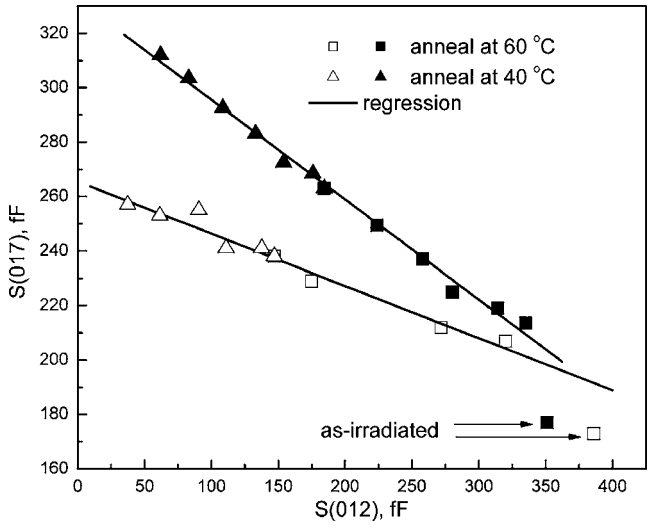

FIG. 5. Regression analysis of the growth of the E1 trap and loss of the E0 trap during two-step annealing at 40 and 60 °C for ⟨111⟩ (filled symbols) and ⟨100⟩ (empty symbols) detectors. The DLTS signal was measured at a bias voltage of −10 V. The filling pulse amplitude was 5 V.

The difference between the slopes of the two regression lines is an indication of different ratios between the C_s and O_i concentrations in the two materials [see Eq. (9)]. Following from the data presented in Fig. 5 the ⟨111⟩ diodes have about twice the ratio of carbon to oxygen concentrations as compared to the ⟨100⟩ diodes. However, the values of τ_{CC}^{-1} are practically the same for both types of diodes. This is an evidence for a similar carbon content in ⟨111⟩ and ⟨100⟩ wafers.

The absolute concentrations of carbon and oxygen in FZ silicon can be determined using previous studies of C_i reactions.[11] To do this it is necessary to know the coefficients K_{CC} and K_{CO}. However, as pointed out earlier, there are controversial data on the absolute values of the coefficients and on the ratio $K_{\mathrm{CC}}/K_{\mathrm{CO}}$ (see Refs. 7 and 11–13). Therefore, this problem requires further studies. In order to evaluate our data we have used K_{CC} and K_{CO}, as given in Ref. 11.

According to Ref. 11 for impurity concentrations $[C_S]=[O_i]=10^{16}$ cm^{-3} in n-type silicon, the values of partial inverse annealing times are

$$\tau_{\mathrm{CC}}^{-1}=4.5\times10^{7}\exp\left(-\frac{0.77\ \mathrm{eV}}{k_BT}\right)\ \mathrm{s}^{-1}, \tag{13}$$

$$\tau_{\mathrm{CO}}^{-1}=1.35\times10^{8}\exp\left(-\frac{0.77\ \mathrm{eV}}{k_BT}\right)\ \mathrm{s}^{-1}. \tag{14}$$

They obey the Arrhenius law with the activation energy of C_i annealing which is consistent with our data and results of other works.[9,10] It should also be noted that the extraction of τ_{ann}^{-1} and η from the data presented in Ref. 10 gives a τ_{CC}^{-1} very close to the values expressed by Eq. (13).

Using Eqs. (9)–(11), (13), and (14), we can determine the carbon and oxygen contents in our diodes. At a depth of more than 50 μm from the surface both ⟨100⟩ and ⟨111⟩ diodes contain a similar carbon concentration of about 1.5×10^{15} cm^{-3}. However, the oxygen content at the same depth is different. We have obtained $[O]=2.5\times10^{15}$ cm^{-3} for ⟨100⟩ diodes and $[O]=1\times10^{15}$ cm^{-3} for ⟨111⟩ diodes.

It is evident that the suggested method allows us to determine rather low contents of carbon and oxygen impurities in silicon when SIMS and IR-absorption methods are ineffective. The only limitation is the ratio between concentrations of carbon (or oxygen) and shallow donors. For "detector-grade" silicon carbon concentrations down to about 10^{13}–10^{14} cm^{-3} can be measured.

V. DISCUSSION

There are some consequences of the inhomogeneous depth distribution of C_i annealing rates. First, studies of the C_i annealing rate at different depths can help to trace impurity distribution in fully processed detector structures. Therefore, the studies of C_i annealing could be useful to optimize detector processing.

Another consequence is related to the interpretation of DLTS data of minority traps in n-type structures. In Ref. 9 it has been shown that in detectors irradiated with α particles the final value of the DLTS peak amplitude related to the H2

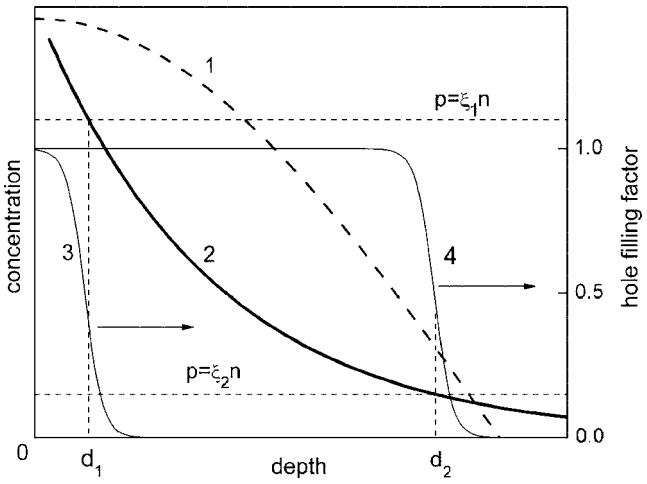

FIG. 6. Schematic drawing of defect (1) and injected hole (2) distributions during a voltage pulse applied to α-irradiated p-n junction. The ratios of $c_p/c_n=\xi^{-1}$ for H1(C_i) and H2(C_iO_i) traps are different, resulting in the fact that the defects will only be filed with holes after the injection pulse when p/n is higher than ξ_1 or ξ_2, respectively. Therefore, the donor levels of C_i will be filled with holes at $0<x<d_1$, while C_iO_i will be filled with holes at $0<x<d_2$. In these regions their hole filling factors defined by Eq. (16) are close to 1 (curve 3 for C_i and curve 4 for C_iO_i).

trap (C_iO_i) was higher than the initial value of the H1 peak amplitude (C_i). This would mean that only a part of the C_iO_i complex forms from the disappeared C_i. Another feature of the C_i annealing process found in Ref. 9 was the observation that there is some delay in the additional growth of the H2 trap and the rate of the H2 peak growth after a complete disappearance of the H1 peak depends on the conditions of diode processing. In our opinion these data can, however, be explained by taking into account the inhomogeneous distribution of the C_i annealing rate and the different ratios between minority (c_p) and majority (c_n) carrier capture coefficients for the H1 and H2 traps.

As has been indicated in Ref. 9, the depth of radiation induced defect formation under ^{238}Pu irradiation is 25 μm. This value is consistent with data presented in Ref. 20. However, when a surface source of α particles is used, a inhomogeneous depth distribution of radiation damage with a more damaged region near the surface of the structures is produced (see curve 1 in Fig. 6). The implantation dose of He used in Ref. 9 was 1×10^9 cm^{-2}. Following from available experimental results,[21] the radiation defect density at a depth of $\leqslant5$ μm is expected to be about 10^{13} cm^{-3}. Using known[22] capture cross sections of holes by the oxygen-vacancy and divacancy defects, we can estimate the diffusion length of holes to be about 5 μm. Therefore, one can expect that the hole concentration during steady-state injection pulses decreases 50–100 times along the damaged region (see curve 2 in Fig. 6).

This high recombination rate is very important when we determine the concentration of minority carrier traps with different ratios of capture coefficients of electrons and holes $\xi=c_n/c_p$. Under the steady-state injection condition the filling of an ith trap with holes can be written as[23,24]

$$N_{Tpi}=N_{Ti}\frac{c_{pi}p}{c_{pi}p+c_{ni}n}=N_{Ti}f_{pi}, \tag{15}$$

where N_{Ti} is the concentration on the ith trap, c_{ni} and c_{pi} are electron and hole capture coefficients, and f_{pi} is the hole filling factor which can be written as

$$f_{pi}=\frac{1}{1+\xi_i(n/p)}, \tag{16}$$

with $\xi_i=c_{ni}/c_{pi}$. A minority trap will be filled by holes in the p^+-n diode region where $\xi_i(n/p)\ll1$ and empty in the region where $\xi_i(n/p)\gg1$. This is why only traps situated in the region with $\xi<p/n$ will contribute to DLTS signals. Therefore, defects with a higher ratio of c_p/c_n can exhibit larger DLTS signals for two reasons. First, the fraction of traps occupied with holes is higher at the same injection current and, second, the depths up to which defects are occupied by a minority carrier pulse is wider (see curves 3 and 4 in Fig. 6). Values published earlier are for C_iO_i (H2 trap), $c_p/c_n\geqslant90$ at $T=185$ K (see Refs. 14 and 22), and for C_i (for the H1 trap): $c_p/c_n\approx4$ (see Ref. 14). This could mean that in the α-particle irradiated structures[9] the DLTS signal of the H2 trap had been observed up to greater depths than the DLTS signal of the H1 trap. Furthermore, since the annealing of the C_i (H1) trap is delayed at greater depths the interpretation of the DLTS signals becomes particularly difficult and might lead to wrong interpretations as, for example, a statement that the annealing of C_i does not coincide with the growth of C_iO_i.

However, another explanation of the delayed appearance of the C_iO_i complex has previously been reported. It is related to the formation of the C_iO_i precursor which was labeled $C_iO_i^*$ in Ref. 25. The existence of this complex has been evidenced both by IR measurements[19] and by DLTS data.[18,25–27] As has been shown in Refs. 18 and 25–27, not all C_i atoms form directly C_iO_i complexes. A fraction of C_i is kept in the form of $C_iO_i^*$ complexes which only afterwards transform into the stable C_iO_i configuration.

The energy level of $C_iO_i^*$ is about $E_v+0.34$ eV, which is only about 0.02 eV less than the energy level of C_iO_i. However, it is enough to distinguish these defects from each other.[23–25] There is no evidence for the formation of $C_iO_i^*$ obtained by DLTS in n-Si. It was observed only in p-type diodes.[23–25] According to Refs. 18 and 27, the rate of $C_iO_i^*\rightarrow C_iO_i$ transformation should be independent of the impurity content. Furthermore, the sum of all carbon related defect concentrations is constant: $[C_i]+[C_iO_i^*]+[C_iO_i]=[C_i]_{\text{initial}}$. These two statements contradict the experimental data presented in Ref. 9 and allow us to reject the $C_iO_i^*\rightarrow C_iO_i$ transformation as reason for the delayed growth of C_iO_i reported in Ref. 9 for Si detectors.

In any case, our results are consistent with the second assumption given in the Introduction, that it is only carbon interstitial atoms generated by the "Watkins replacement mechanism" that are responsible for the formation of the carbon related complexes at RT.

VI. CONCLUSION

It has been shown that the rate of interstitial carbon annealing in detectors made of high resistivity silicon depends on the distance from the diode surface. This is first of all caused by an inhomogeneous depth distribution of oxygen in fully processed detectors. We also demonstrated that this fact can strongly influence the interpretation of experimental data obtained with the DLTS method.

Finally, we measured the activation energy for the carbon interstitial migration to be (0.72 ± 0.05) eV and could clearly show that the interstitial carbon reactions can be used to monitor the carbon and oxygen impurity contents and their depth distribution in fully processed detector structures.

ACKNOWLEDGMENTS

This work has been carried out in the framework of the RD50 CERN Collaboration and has been partially supported by INTAS-Belarus, Grant No. 03-50-4529.

[1] B. C. MacEvoy, A. Santocchia, and G. Hall, Physica B **273–274**, 1045 (1999).
[2] B. C. MacEvoy and G. Hall, Mater. Sci. Semicond. Process. **1**, 243 (2000).
[3] F. Moscatelli, A. Santocchia, B. MacEvoy, G. Hall, D. Passeri, M. Petasecca, and G. U. Pignatel, IEEE Trans. Nucl. Sci. **51**, 1759 (2004).
[4] S. Lazanu, I. Lazanu, and M. Bruzzi, Nucl. Instrum. Methods Phys. Res. A **514**, 9 (2003).
[5] I. Lazanu and S. Lazanu, Nucl. Instrum. Methods Phys. Res. B **201**, 491 (2003).
[6] S. Lazanu and I. Lazanu, Phys. Scr. **69**, 376 (2004).
[7] G. Davies, E. C. Lightowlers, R. C. Newman, and A. S. Oates, Semicond. Sci. Technol. **2**, 524 (1987).
[8] G. Davies and R. C. Newman, in *Handbook on Semiconductors*, edited by T. S. Moss (Elsevier Science, Amsterdam, 1994), Vol. 3B, p. 1557.
[9] B. Schmidt, V. Eremin, A. Ivanov, N. Strokan, E. Verbitskaya, and Z. Li, J. Appl. Phys. **76**, 4072 (1994).
[10] L. W. Song, B. W. Benson, and G. D. Watkins, Phys. Rev. B **42**, 5765 (1990).
[11] V. P. Markevich and L. I. Murin, Fiz. Tekh. Poluprovodn. (S.-Peterburg) **22**, 769 (1988) [Sov. Phys. Semicond. **22**, 574 (1988)].
[12] J. L. Benton, M. T. Asom, R. Sauer, and L. C. Kimerling, Mater. Res. Soc. Symp. Proc. **104**, 85 (1988).
[13] L. C. Kimerling, M. T. Asom, J. L. Benton, P. J. Drevinsky, and C. E. Caefer, Mater. Sci. Forum **38–41**, 141 (1989).
[14] M. Moll, Ph.D. thesis, University of Hamburg.
[15] G. Lindström, Nucl. Instrum. Methods Phys. Res. A **512**, 30 (2003).
[16] A. Borghesi, B. Pivac, A. Sassella, and A. Stella, J. Appl. Phys. **77**, 4169 (1995).
[17] A. C. Damask and G. J. Dienes, *Point Defects in Metals* (Gordon and Breach, New York 1963).
[18] B. N. Mukashev, Kh. A. Abdullin, and Yu. V. Gorelkinskǐ, Usp. Fiz. Nauk **170**, 154 (2000) [Phys. Usp. **43**, 139 (2000)].
[19] L. Dobaczewski, A. R. Peaker, and K. Bonde Nielsen, J. Appl. Phys. **96**, 4689 (2004).
[20] V. A. Kozlov and V. V. Kozlovski, Fiz. Tekh. Poluprovodn. (S.-Peterburg) **35**, 769 (2001) [Semiconductors **35**, 735 (2001)].
[21] A. Hallén, N. Keskitalo, F. Masszi, and V. Nágl, J. Appl. Phys. **79**, 3906 (1996).
[22] A. Hallén, B. U. R. Sundquist, Z. Paska, B. G. Svensson, M. Rosling, and J. Tiren, J. Appl. Phys. **67**, 1266 (1990).
[23] A. C. Wang and C. T. Sah, J. Appl. Phys. **57**, 4645 (1985).
[24] P. Blood and J. W. Orton, *The Electrical Characterization of Semiconductors: Majority Carriers and Electron States*, Techniques of Physics Vol. 14, edited by N. H. March (Academic, New York, 1992), Chap. 10.
[25] L. I. Khirunenko *et al.*, in *Gettering and Defect Engineering in Semiconductor Technology XI*, Proceedings of the 11th International Autumn Meeting, Giens, France, 25–30 September 2005, edited by B. Pichaud, A. Claverie, D. Alquier, H. Richter, and M. Kittler (Trans Tech Publications, Switzerland, 2005), pp. 261–266.
[26] C. A. Londos, Semicond. Sci. Technol. **5**, 645 (1990).
[27] Kh. A. Abdullin, B. N. Mukashev, M. F. Tamendarov, and T. B. Tashenov, Phys. Lett. A **144**, 198 (1990).